



ELSEVIER

March 1998

Optical Materials 10 (1998) 9–17



# Spectroscopic properties and laser emission of $\text{Er}^{3+}$ in scandium silicates near $1.5 \mu\text{m}$

L. Fornasiero<sup>\*</sup>, K. Petermann, E. Heumann, G. Huber

*Institut für Laser-Physik, Universität Hamburg, Jungiusstr. 9a, D-20355 Hamburg, Germany*

Received 1 June 1997; revised 17 July 1997; accepted 4 September 1997

## Abstract

We have grown  $\text{Er}^{3+}$ - and  $\text{Er}^{3+}$ -,  $\text{Yb}^{3+}$ -doped scandium silicates  $\text{Sc}_2\text{SiO}_5$  and  $\text{Sc}_2\text{Si}_2\text{O}_7$  by the Czochralski technique and analyzed the spectroscopic properties of these crystals. Crystal data of the host materials, the lifetimes and the Stark level splitting of the Er energy levels as well as laser parameters of samples pumped by a  $\text{Ti}:\text{Al}_2\text{O}_3$ -laser and InGaAs-laser diodes are presented. Laser oscillation of diode pumped Er,Yb: $\text{Sc}_2\text{SiO}_5$  yielded a slope efficiency of 2.4% and a maximum output power of 24 mW. © 1998 Elsevier Science B.V.

PACS: 42.70; 42.55.R

## 1. Introduction

Applications in opto-communication and LIDAR systems motivate the realization of an efficient eye-safe laser emitting at  $1.55 \mu\text{m}$ . A concept for a coherent radiation source with high beam quality in this spectral region is the stimulation of  ${}^4\text{I}_{13/2} \rightarrow {}^4\text{I}_{15/2}$  transitions of  $\text{Er}^{3+}$ -ions in solid-state materials as three or quasi three level laser.

For the possible use of powerful InGaAs diodes the Er doped materials are often codoped with  $\text{Yb}^{3+}$ -ions and pumped into the broad Yb  ${}^4\text{F}_{5/2}$  absorption band around 970 nm. In this scheme most of the energy of the excited Yb-ions is transferred to the Er-ions by dipole–dipole interaction exciting

them to the  ${}^4\text{I}_{11/2}$  manifold which decays mainly into the upper laser level  ${}^4\text{I}_{13/2}$  (see Fig. 1). The lower laser level within the  ${}^4\text{I}_{15/2}$  ground state is thermally populated. This results in reabsorption losses and in comparison to four level systems in a higher laser threshold.

The Yb codoped three level  $1.55 \mu\text{m}$  Er laser works well within phosphate glass bulk [1–3] and silica fiber lasers [4] with slope efficiencies up to tens of percent. The favorable laser characteristics of the phosphate glasses are due to a high Yb–Er energy transfer efficiency [5,6], low upconversion losses, and better transmission through thin optimized microchip samples.

Laser action in crystalline hosts around  $1.55 \mu\text{m}$  have to our knowledge been reported for Er,Yb:YAG [7,8], Er,Yb: $\text{Y}_2\text{SiO}_5$  [8–10], Er,Yb: $\text{Ca}_2\text{Al}_2\text{SiO}_7$  [11,12] and Er,Yb: $\text{SrY}_4(\text{SiO}_4)_3\text{O}$  [13]. Some data of

<sup>\*</sup> Corresponding author. Tel.: +49 40 41235241; fax: +49 40 41236281; e-mail: fornasio@physnet.uni-hamburg.de.

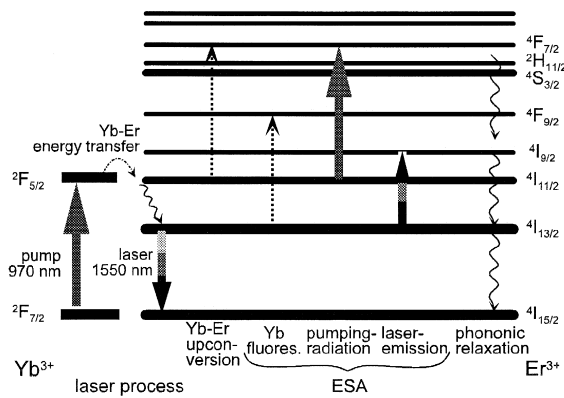


Fig. 1. Inter- and intraionic processes within an Yb codoped 1.55  $\mu\text{m}$  Er laser.

these lasers are presented in Table 1. The slope efficiencies of the crystalline lasers are still far below the corresponding values in phosphate glass samples. This is mostly due to upconversion processes from the  $^4I_{11/2}$  manifold nourished by pumping and laser radiation. Ref. [7] reports a slope efficiency  $\eta_{\text{diff}} = 50\%$  in Er:YAG pumped directly into the  $^4I_{13/2}$  manifold by short pulses of an Er:glass laser at 1535 nm where pump excited state absorption is negligible. This result can be compared with  $\eta_{\text{diff}} = 7\%$  quoted in Ref. [8] when Er,Yb:YAG is pumped into the Yb absorption band at 970 nm and subsequent energy transfer into the Er  $^4I_{11/2}$  manifold is exploited.

Upconversion losses and excited state absorption should be diminished in materials with high effective phonon energies where the phonon assisted nonradiative decay rate of the excited Er  $^4I_{11/2}$  manifold into

the upper laser level  $^4I_{13/2}$  is enhanced. This is the reason why among the crystalline Er 1.55  $\mu\text{m}$  lasers are various silicates whose effective phonon energies are high (about  $1000\text{ cm}^{-1}$ ) due to the vibration modes of the Si–O bond. The high effective phonon energy in combination with a presumed high Stark splitting motivated us to test the hosts  $\text{Sc}_2\text{SiO}_5$  and  $\text{Sc}_2\text{Si}_2\text{O}_7$ . These materials were firstly used by Tkachuk et al. with Nd doping [14] but had to our knowledge never been investigated with other dopants.

## 2. Crystals

The orthosilicate  $\text{Sc}_2\text{SiO}_5$  is a monoclinic crystal isostructural to  $\text{Y}_2\text{SiO}_5$  with space group  $C_{2h}^6$ . The silicon ions are surrounded by four oxygen neighbors forming a tetrahedron. The scandium ions are sixfold coordinated and reside on two lattice sites with slightly different octahedral structure in  $C_1$  site symmetry.

The different spectroscopic behavior of rare earth dopants in  $\text{Sc}_2\text{SiO}_5$  and  $\text{Y}_2\text{SiO}_5$  is due to the smaller size of the scandium ions (ionic radius =  $0.75\text{ \AA}$  in sixfold coordination) with respect to the yttrium ions (ionic radius =  $0.90\text{ \AA}$ ) resulting in an enhanced crystal field strength for dopants at the Sc site. This can increase the Stark-splitting of the thermally populated Er ground state as well as of the other electronic energy levels and therefore reduce reabsorption losses.

Table 1

Parameters of Yb codoped 1.5  $\mu\text{m}$  Er: YAG and Er:  $\text{Y}_2\text{SiO}_5$  lasers. Slope efficiencies and thresholds refer to the absorbed pump power

	Er,Yb:YAG	Er,Yb: $\text{Y}_2\text{SiO}_5$	Er,Yb: $\text{Ca}_2\text{Al}_2\text{SiO}_7$	Er,Yb: $\text{SrY}_4(\text{SiO}_4)_3\text{O}$
Stark splitting of Er $^4I_{15/2}$	$573\text{ cm}^{-1}$	$478.5\text{ cm}^{-1}$	$460\text{ cm}^{-1}$	
Decay time of Er $^4I_{11/2}$	$100\text{ }\mu\text{s}$	$18\text{ }\mu\text{s}$	$41\text{ }\mu\text{s}$	$13\text{ }\mu\text{s}$
Decay time of Er $^4I_{13/2}$	$7.7\text{ ms}$	$6\text{ ms}$	$7.6\text{ ms}$	$6\text{ ms}$
Peak emission cross section of $^4I_{13/2} \rightarrow ^4I_{15/2}$	$15 \times 10^{-21}\text{ cm}^2$	$8 \times 10^{-21}\text{ cm}^2$	$8 \times 10^{-21}\text{ cm}^2$	$13 \times 10^{-21}\text{ cm}^2$
Laser performance	InGaAs-diode pumped, $P_{\text{th}} = 46\text{ mW}$ , $\eta = 7\%$ at $1646\text{ nm}$	InGaAs-diode pumped, $P_{\text{th}} = 61\text{ mW}$ , $\eta = 5.6\%$ at $1617\text{ nm}$	Ti: $\text{Al}_2\text{O}_3$ pumped, $P_{\text{th}} = 90\text{ mW}$ , $\eta = 2.7\%$ at $1555\text{ nm}$	InGaAs-diode pumped, $P_{\text{th}} = 274\text{ mW}$ , $\eta = 0.4\%$ at $1554\text{ nm}$
Refs.	[7,8]	[8–10]	[11,12]	[13]

Table 2  
Structural data of  $\text{Sc}_2\text{SiO}_5$  and  $\text{Sc}_2\text{Si}_2\text{O}_7$

	$\text{Sc}_2\text{Si}_2\text{O}_7$	$\text{Sc}_2\text{SiO}_5$
Crystal system	monoclinic	monoclinic
Space group (Schoenflies)	$\text{C}_{2h}^3$	$\text{C}_{2h}^6$
Lattice constants	$a = 6.56 \text{ \AA}, b = 8.58 \text{ \AA}, c = 4.74 \text{ \AA}, \beta = 103.8^\circ$	$a = 12.05 \text{ \AA}, b = 6.43 \text{ \AA}, c = 9.97 \text{ \AA}, \beta = 103.9^\circ$
Volume of unit cell	$259.8 \text{ \AA}^3$	$749.8 \text{ \AA}^3$
Formulars per unit cell Z	2	8
Density of cations	$1.54 \times 10^{22} \text{ cm}^{-3}$	$2.13 \times 10^{22} \text{ cm}^{-3}$
Density	$3.39 \text{ g/cm}$	$3.52 \text{ g/cm}$
Melting point	$1960^\circ\text{C}$	$1920^\circ\text{C}$
Phonon energy	$700\text{--}1200 \text{ cm}^{-1}$	$750\text{--}1200 \text{ cm}^{-1}$
Refractive indices (at 632.8 nm)	$n_x = 1.75, n_y = 1.78, n_z = 1.80$	$n_x = 1.82, n_y = 1.84, n_z = 1.86$
Number of potential Er sites	1	2 (only 1 occupied)
Symmetry of Er site	$\text{C}_2$	$\text{C}_1$

$\text{Sc}_2\text{Si}_2\text{O}_7$  crystallizes in the thortveitite structure (space group  $\text{C}_{2h}^3$ ). The sixfold coordinated scandium ions reside within one type of oxygen octahedra with site symmetry  $\text{C}_2$ .

The investigated crystals were grown by the Czochralski technique at our institute. Boules of  $\text{Sc}_2\text{SiO}_5$  were produced with  $[\text{Er}(1.3 \times 10^{20} \text{ cm}^{-3})]$ ,  $[\text{Yb}(7.7 \times 10^{20} \text{ cm}^{-3}), \text{Er}(4.7 \times 10^{19} \text{ cm}^{-3})]$ , and  $[\text{Yb}(7.7 \times 10^{20} \text{ cm}^{-3}), \text{Er}(3.0 \times 10^{19} \text{ cm}^{-3})]$  doping. The crystals had a length of 15 mm, a diameter of about 8 mm and were of good optical quality.

The Yb distribution coefficient was determined by microprobe analysis to be nearly  $k_{\text{Yb}} \approx 1$ . The distribution coefficient of Er is  $k_{\text{Er}} \approx 0.6$ . The small distribution coefficient combined with a narrow linewidth of the absorption spectra at 10 K indicate that the Er-ions prefer only one of the two Sc-sites.

$\text{Sc}_2\text{Si}_2\text{O}_7$  crystals were grown with  $[\text{Er}(7.7 \times 10^{19} \text{ cm}^{-3})]$ ,  $[\text{Yb}(4.2 \times 10^{20} \text{ cm}^{-3}), \text{Er}(1.9 \times 10^{19} \text{ cm}^{-3})]$  and  $[\text{Yb}(8.8 \times 10^{20} \text{ cm}^{-3}), \text{Er}(7.7 \times 10^{19} \text{ cm}^{-3})]$  doping. The distribution coefficients are about  $k_{\text{Er}} \approx 0.5$  and  $k_{\text{Yb}} \approx 0.7$ .

While the structure of  $\text{Sc}_2\text{Si}_2\text{O}_7$  is well known [15] an investigation by the Debye–Scherrer method had to be performed to get precise information about  $\text{Sc}_2\text{SiO}_5$  [16].

Additionally, the refractive indices along the optical axes were calculated for both hosts from measurements of the Brewster-angles at 632 nm and the signs X, Y and Z were given to the indicatrix axes in sequence of increasing refractive index.

The structural data of the silicates are summarized in Table 2.

### 3. Absorption and emission cross sections

The absorption of crystal samples was measured by a spectrophotometer (Varian Cary 2400). In order to determine the emission spectra of Er doped crystals, we pumped the  $^2\text{H}_{11/2}$  manifold with an argon-ion-laser at 488 nm and detected the fluorescence light by a Fourier transform spectrometer (Biorad FTS 60).

The effective emission cross sections at 300 K were calculated from the absorption cross sections by using the reciprocity method. The shape of each emission cross section spectrum was confirmed by comparison with the spectrum derived from the formula of Füchtbauer and Ladenburg from the corresponding fluorescence spectrum. This procedure is described elsewhere [17,18].

The Yb codoped crystals absorb the pumping beam efficiently between 900 and 1000 nm with two peaks at 920 and 978 nm in both scandium silicates as shown in Fig. 2.

The peak effective absorption cross sections of Er on the transition  $^4\text{I}_{15/2} \rightarrow ^4\text{I}_{13/2}$  are presented in Fig. 3. They are about  $1.5 \times 10^{-20} \text{ cm}^2$  in  $\text{Sc}_2\text{SiO}_5$  and for one line even  $4.0 \times 10^{-20} \text{ cm}^2$  in  $\text{Sc}_2\text{Si}_2\text{O}_7$ . The peak emission cross sections in  $\text{Sc}_2\text{Si}_2\text{O}_7$  are much higher than the peak emission cross sections in

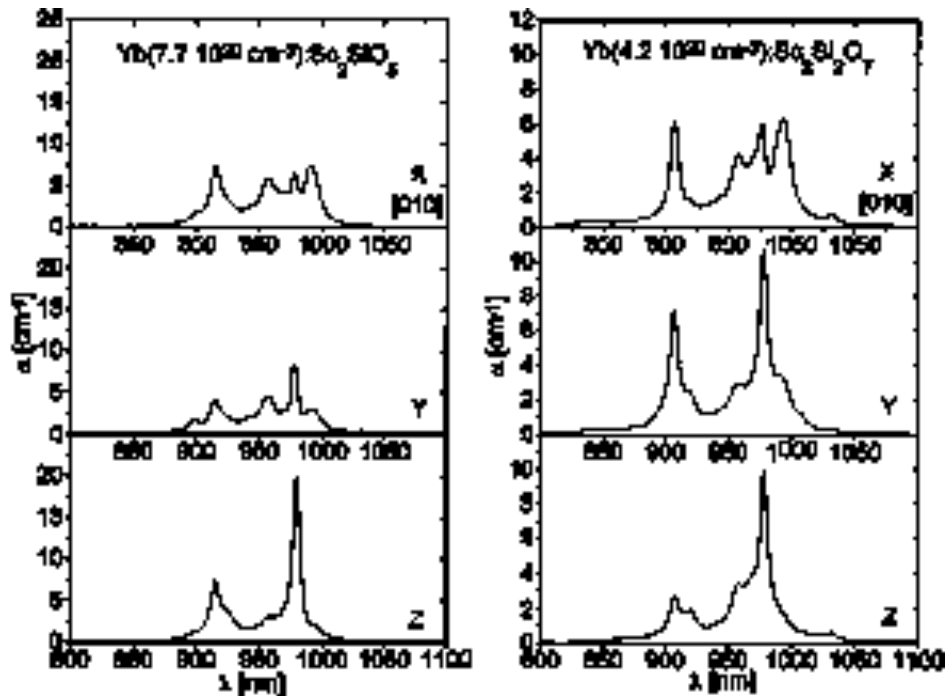


Fig. 2. Absorption of  $\text{Yb}(7.7 \times 10^{20} \text{ cm}^{-3})\text{:Sc}_2\text{SiO}_5$  (left) and  $\text{Yb}(4.2 \times 10^{20} \text{ cm}^{-3})\text{:Sc}_2\text{Si}_2\text{O}_7$  (right).

Er:YAG ( $1.5 \times 10^{-20} \text{ cm}^2$ ), Er: $\text{Y}_2\text{SiO}_5$  ( $0.8 \times 10^{-20} \text{ cm}^2$ ), Er: $\text{Ca}_2\text{Al}_2\text{SiO}_7$  ( $0.8 \times 10^{-20} \text{ cm}^2$ ) and Er: $\text{SrY}_4(\text{SiO}_4)_3\text{O}$  ( $1.3 \times 10^{-20} \text{ cm}^2$ ) which are reported in Refs. [8,11,13]. The difference is less distinct for the lines at longer wavelength where inversion is reached first.

#### 4. Energy level scheme

The energies of the Stark levels within the Er manifolds  $^4\text{I}_{9/2}$ ,  $^4\text{I}_{11/2}$ ,  $^4\text{I}_{13/2}$ , and  $^4\text{I}_{15/2}$  were determined by analyzing absorption and fluorescence spectra at 10 K. The results are presented in Table 3. The total splitting of the  $^4\text{I}_{15/2}$  ground state is  $455 \text{ cm}^{-1}$  in  $\text{Sc}_2\text{SiO}_5$  and  $434 \text{ cm}^{-1}$  in  $\text{Sc}_2\text{Si}_2\text{O}_7$  and is less than in Er:YAG ( $568 \text{ cm}^{-1}$ ), Er: $\text{Y}_2\text{SiO}_5$  ( $479 \text{ cm}^{-1}$ ) and Er: $\text{Ca}_2\text{Al}_2\text{SiO}_7$  ( $460 \text{ cm}^{-1}$ ). Furthermore only one set of lines was observed in  $\text{Sc}_2\text{SiO}_5$  indicating that the erbium ions presumably occupy only one of the two different scandium sites.

According to the symmetry of the potential Er sites ( $\text{C}_2$ -symmetry in  $\text{Sc}_2\text{Si}_2\text{O}_7$  and  $\text{C}_1$  in  $\text{Sc}_2\text{SiO}_5$ )

a splitting into  $J + 1/2$  Stark components of each manifold is expected. However, in  $\text{Sc}_2\text{Si}_2\text{O}_7$  only 7 instead of 8 fluorescence lines could be determined on the transition  $^4\text{I}_{13/2} \rightarrow ^4\text{I}_{15/2}$ . The reason for this lack of one line may be accidental degeneracy of two Stark levels in the  $^4\text{I}_{15/2}$  manifold.

#### 5. Lifetimes

In order to determine the decay time of the  $\text{Er}^{3+}$ -manifolds we excited the crystals at 518 nm with an optical parametric oscillator (manufactured by GWU with a BBO-crystal) pumped by a frequency tripled Nd:YAG laser. The pulse duration was about 20 ns. The fluorescence signals were discriminated with a monochromator and detected by a photomultiplier with S1 characteristic and a Ge-detector in the visible and infrared region, respectively. The response times of the pure detectors were about some nanoseconds while attention was kept that in each measurement the response time of the combined capacity and resistance of the detector and the

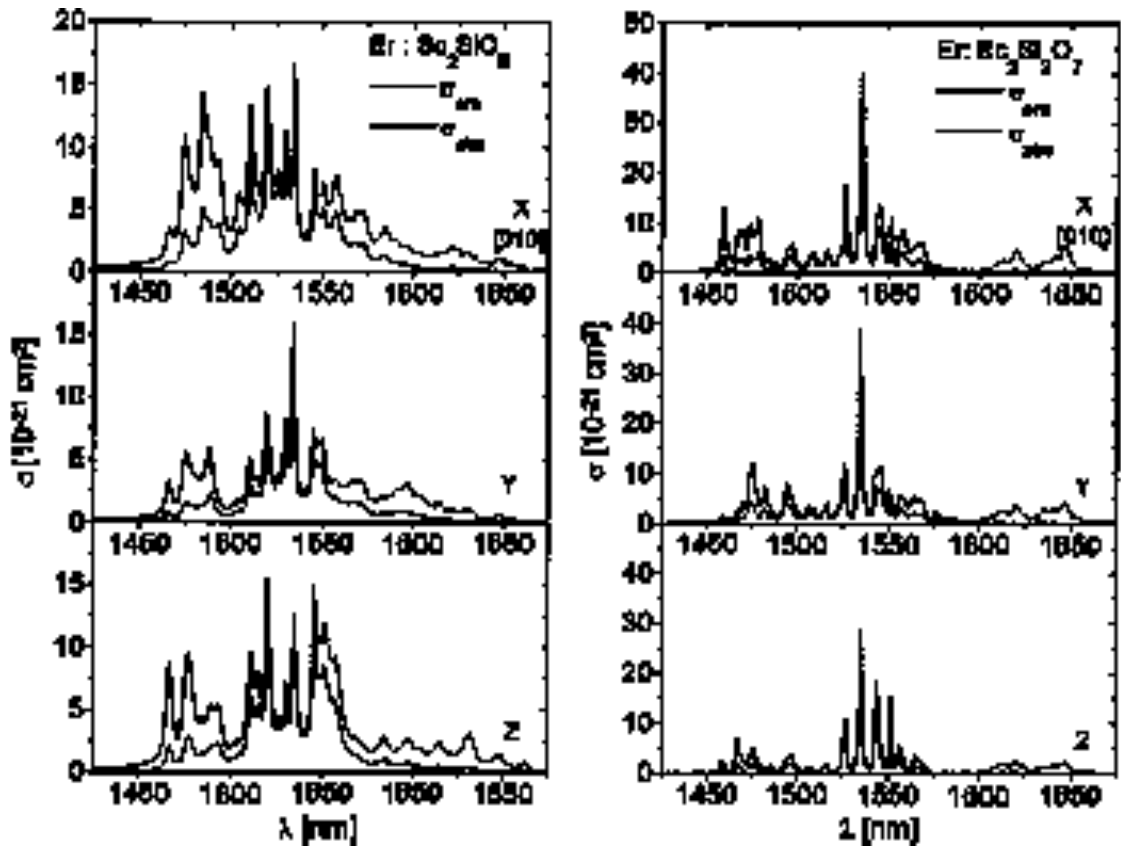


Fig. 3. Near-infrared effective absorption (full line) and emission cross sections (dotted line) of the  ${}^4I_{15/2} \leftrightarrow {}^4I_{13/2}$  transition in  $\text{Er}(1.3 \times 10^{20} \text{ cm}^{-3})\text{:Sc}_2\text{SiO}_5$  (left column) and  $\text{Er}(7.7 \times 10^{19} \text{ cm}^{-3})\text{:Sc}_2\text{Si}_2\text{O}_7$  (right column) in X, Y and Z-polarization at 300 K.

oscilloscope was less than 5% of the measured decay time.

The data were stored in an oscilloscope (LeCroy 9360) and added for several hundred exciting cycles. The fluorescence rise and the decay times were assigned to the electronic lifetimes in the participating manifolds as explained in Ref. [19].

The Er lifetimes in low doped scandium silicate hosts are shown in Table 4. The lifetimes of the  ${}^4I_{13/2}$  manifold compare with the corresponding values in other silicates (see Table 1) while the decay times of the  ${}^4I_{11/2}$  manifold are the shortest to our knowledge known within any crystalline  $1.55 \mu\text{m}$  Er laser.

Table 3

Energies of the  $\text{Er}^{3+}$  Stark levels in the scandium silicates in  $\text{cm}^{-1}$ . Because in  $\text{Sc}_2\text{Si}_2\text{O}_7$  only 7 instead of 8 expected fluorescence lines of the transition  ${}^4I_{13/2} \rightarrow {}^4I_{15/2}$  are observed at 10 K, the energy of one Stark level in the manifold  ${}^4I_{15/2}$  is uncertain

	$\text{Sc}_2\text{Si}_2\text{O}_7$	$\text{Sc}_2\text{SiO}_5$
${}^4I_{15/2}$	0, 39, 70, 126, 180, 417, 434	0, 48, 72, 165, 212, 362, 391, 455
${}^4I_{13/2}$	6513, 6548, 6594, 6640, 6804, 6815, 6855	6518, 6584, 6624, 6653, 6768, 6786, 6824
${}^4I_{11/2}$	10200, 10233, 10270, 10337, 10374, 10378	10205, 10260, 10281, 10323, 10351, 10364
${}^4I_{9/2}$	12370, 12481, 12550, 12590, 12648	12374, 12454, 12539, 12585, 12646

Table 4

Lifetimes of the excited manifolds of the  $\text{Er}^{3+}$ -ion in  $\text{Er}(1.3 \times 10^{20} \text{ cm}^{-3})\text{:Sc}_2\text{SiO}_5$  and  $\text{Er}(7.7 \times 10^{19} \text{ cm}^{-3})\text{:Sc}_2\text{Si}_2\text{O}_7$

	$\text{Sc}_2\text{Si}_2\text{O}_7$	$\text{Sc}_2\text{SiO}_5$
$^4\text{S}_{3/2}$	820 ns	1.8 $\mu\text{s}$
$^4\text{I}_{9/2}$	70 ns	100 ns
$^4\text{I}_{11/2}$	5.6 $\mu\text{s}$	8.9 $\mu\text{s}$
$^4\text{I}_{13/2}$	6.6 ms	5.6 ms

To ascertain the transfer efficiencies from the Yb-ions to the Er-ions we measured the fluorescence decay time of the Yb ions excited at 940 nm and its quenching in the presence of Er acceptors. The transfer efficiency is 68% in  $\text{Yb}(7.7 \times 10^{20} \text{ cm}^{-3})$ ,  $\text{Er}(3.0 \times 10^{19} \text{ cm}^{-3})\text{:Sc}_2\text{SiO}_5$ , 75% in  $\text{Yb}(7.7 \times 10^{20} \text{ cm}^{-3})$ ,  $\text{Er}(4.7 \times 10^{19} \text{ cm}^{-3})\text{:Sc}_2\text{SiO}_5$  and 64% in  $\text{Yb}(4.2 \times 10^{20} \text{ cm}^{-3})$ ,  $\text{Er}(1.9 \times 10^{19} \text{ cm}^{-3})\text{:Sc}_2\text{Si}_2\text{O}_7$ .

## 6. Excited state absorption

The excited state absorption (ESA) in  $\text{Er}(1.3 \times 10^{20} \text{ cm}^{-3})\text{:Sc}_2\text{SiO}_5$  and  $\text{Er}(7.7 \times 10^{19} \text{ cm}^{-3})\text{:Sc}_2\text{Si}_2\text{O}_7$  was measured with a pump and probe technique employing a double modulation scheme as explained in Refs. [20–22].

The crystal is mounted on a pinhole and pumped at 488 nm by the slowly chopped beam of an Ar-laser ( $f_{\text{pump}} = 10 \text{ Hz}$ ). Simultaneously, the transmission of light emitted by a halogen lamp is detected. If the Ar-laser beam is switched off, the absorption of the transmitted probe light results exclusively from the ground state (GSA). The detected signal during this cycle is  $I_{\text{np}}$ . If the pump beam is switched on, stimulated emission (SE) and absorption from excited states (ESA) can be detected besides GSA. The intensity of the probe light is  $I_p$ . The change of the signal  $\Delta I = I_p - I_{\text{np}}$ , that is correlated to the chopped

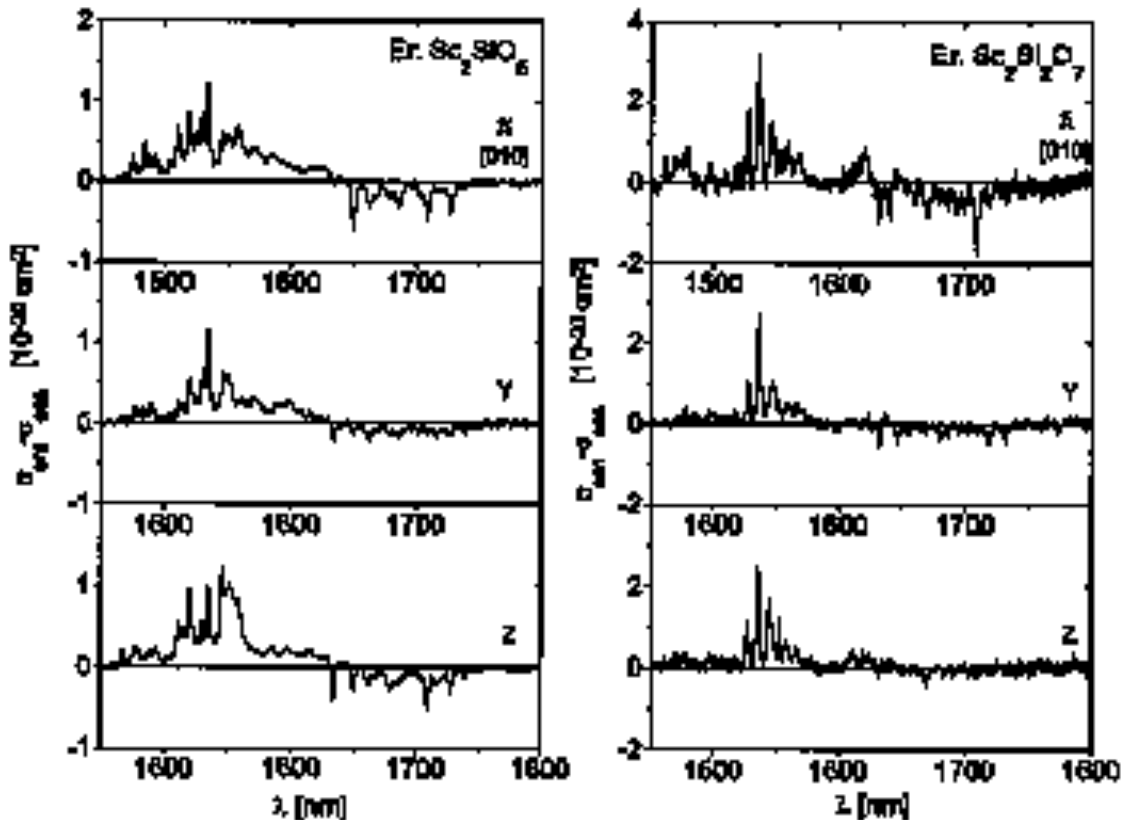


Fig. 4. Stimulated emission-ESA cross sections of  $\text{Er}^{3+}$  in  $\text{Sc}_2\text{Si}_2\text{O}_7$  (right) and  $\text{Sc}_2\text{SiO}_5$  (left).

pump beam, was measured with a second lock-in amplifier using the output of the first lock-in amplifier as input and  $f_{\text{pump}}$  as trigger signal. A computer stores the data and performs further processing.

The change of the signal  $\Delta I$  is a function of the population densities, of the stimulated emission and ESA cross sections  $\sigma_{\text{SE}}^i$ ,  $\sigma_{\text{ESA}}^i$  of the state  $i$ , and of the absorption cross section  $\sigma_{\text{GSA}}$  [22]:

$$\frac{\Delta I}{I_{\text{np}}} \approx \ln\left(\frac{I_{\text{p}}}{I_{\text{np}}}\right) = d\left(\sigma_{\text{GSA}}(\lambda)n_{\text{e}} + \sum_i (\sigma_{\text{SE}}^i(\lambda) - \sigma_{\text{ESA}}^i(\lambda))n_i\right). \quad (1)$$

In this formula  $n_i$  is the population density in an excited state  $i$ ,  $n_{\text{e}} = \sum n_i$  the total density of excited ions, and  $d$  the thickness of the sample. The ground state absorption cross section  $\sigma_{\text{GSA}}$  can be calculated from  $I_{\text{np}}$  if a reference spectrum without crystal has been taken. Fitting the data obtained by formula (1) to  $\sigma_{\text{GSA}}(\lambda)$  in spectral regions where no ESA and only weak stimulated emission are expected yields the proportion of ground state bleaching and a correct value for  $n_{\text{e}}$ .

According to the lifetimes of the different Er states (see Section 5) it can be assumed that nearly all excited ions are in the  $^4\text{I}_{13/2}$  manifold and  $n_{\text{e}} = \sum n_i \approx n(^4\text{I}_{13/2})$  is a good approximation. On this basis the difference  $\sigma_{\text{SE}} - \sigma_{\text{ESA}}$  can be determined.

For possible ESA transitions in a 1.55  $\mu\text{m}$  Yb,Er laser see Fig. 1 in Section 1. In our measurements no ESA could be detected around 970 nm. This is the interesting wavelength region for diode pumping into the Er  $^4\text{I}_{11/2}$  manifold. The absence of ESA in this spectral region is in agreement with the short lifetimes (5.6 and 8.9  $\mu\text{s}$ ) and corresponding low population of the  $^4\text{I}_{11/2}$  manifold in the scandium silicates. In the spectra of Er:Y<sub>2</sub>SiO<sub>5</sub> presented in Ref. [8] a weak ESA was observed between 1050 nm and 1100 nm. The decay time of the  $^4\text{I}_{11/2}$  manifold in this material (16  $\mu\text{s}$ ) is a little bit longer than in the scandium silicates. However, strong ESA in this spectral region is reported for the low phonon energy fluoride Er:YLF where the Er  $^4\text{I}_{11/2}$  decay time is 4 ms making the material suitable for upconversion lasers [23,24].

Although no ESA was detected in the region of InGaAs diode emission and Yb fluorescence we

assume the presence of two ion Yb–Er upconversion processes [ $\text{Yb } ^2\text{F}_{5/2}$ , Er  $^4\text{I}_{11/2}$ ]  $\rightarrow$  [ $\text{Yb } ^2\text{F}_{7/2}$ , Er  $^4\text{F}_{7/2}$ ] and of other cooperative processes as they can be recognized during laser experiments by a weak green fluorescence in the pump channel. Further research has to be done to determine the corresponding upconversion process and parameters.

Measurements in the region of the potential laser wavelength around 1.55  $\mu\text{m}$  (Fig. 4) show ESA from the  $^4\text{I}_{13/2}$  into the  $^4\text{I}_{9/2}$  manifold. The corresponding upconversion process is used in Er:YSGG, Er:BaY<sub>2</sub>F<sub>8</sub>, and other 3  $\mu\text{m}$  lasers to depopulate the lower laser level [25,26].

The presented spectra result from the superimposed effects of stimulated emission (positive cross sections) and ESA (negative cross sections). ESA is detected above 1620 nm. This is in agreement with the energies of the contributing Stark levels of the  $^4\text{I}_{13/2}$  and the  $^4\text{I}_{9/2}$  manifolds ascertained in the low temperature absorption and fluorescence measurements. The absorption from excited states between 1620 and 1750 nm does exclude effective gain and laser action in this wavelength region.

## 7. Laser performance

### 7.1. Excitation by Ti:Al<sub>2</sub>O<sub>3</sub>-laser

The laser performance of the crystals was first tested with a Ti:Al<sub>2</sub>O<sub>3</sub>-laser in a longitudinal pumping scheme. The crystals were mounted within a nearly concentric resonator with mirror radii of  $r = 50$  mm. Purely Er doped samples were pumped at 978 nm into the  $^4\text{I}_{11/2}$  manifold. The pump beam was focused by a lens ( $f = 50$  mm) to a waist of  $\omega_{\text{p}} = 15$   $\mu\text{m}$ . The focusing lens as well as the crystal and the cavity were adjusted to get a suitable overlap between the pump channel and the laser mode and to reach a maximum output power. A low power cw laser emission ( $\approx 1$  mW) on the transition  $^4\text{I}_{13/2} \rightarrow ^4\text{I}_{15/2}$  was achieved in both Er( $1.3 \times 10^{20}$  cm<sup>-3</sup>):Sc<sub>2</sub>SiO<sub>5</sub> and Er( $7.7 \times 10^{19}$  cm<sup>-3</sup>):Sc<sub>2</sub>Si<sub>2</sub>O<sub>7</sub> crystals although the low absorption of the pump light by the  $^4\text{I}_{11/2}$  manifold limited the laser performance.

The Yb codoped crystals generally performed better in the laser experiments than purely Er doped

Table 5

Results of the laser experiments performed with scandium silicates pumped by a Ti:Al<sub>2</sub>O<sub>3</sub> laser. The presented data refer to the best efficiency reached with each crystal and to the absorbed pump power

Crystal	Length (mm)	$\lambda_{\text{pump}}$ (nm)	Pump polarization	Absorbed pump power (%)	$\lambda_{\text{laser}}$ (nm)	Laser polarization	Transmission of output coupler (%)	$P_{\text{thr}}$ (mW)	$\eta_{\text{diff}}$ (%)
Er( $1.3 \times 10^{20} \text{ cm}^{-3}$ ):Sc <sub>2</sub> SiO <sub>5</sub>	1.2	979	X		1558	X	1	≈ 1000	
Er( $3.0 \times 10^{19} \text{ cm}^{-3}$ ), Yb( $7.7 \times 10^{20} \text{ cm}^{-3}$ ):Sc <sub>2</sub> SiO <sub>5</sub>	2.0	920	Z	59	1551	Z	1	805	1.8
Er( $7.7 \times 10^{19} \text{ cm}^{-3}$ ):Sc <sub>2</sub> Si <sub>2</sub> O <sub>7</sub>	3	980	Y	42	1545	Z	1	390	2.6
Er( $1.9 \times 10^{19} \text{ cm}^{-3}$ ), Yb( $4.2 \times 10^{20} \text{ cm}^{-3}$ ):Sc <sub>2</sub> Si <sub>2</sub> O <sub>7</sub>	1.4	978	Y		1556	Z	1	≈ 1000	
Er( $7.7 \times 10^{19} \text{ cm}^{-3}$ ), Yb( $8.8 \times 10^{20} \text{ cm}^{-3}$ ):Sc <sub>2</sub> Si <sub>2</sub> O <sub>7</sub>	1.9	978	Y	65	1556	Z	1	130	2.3

samples. Table 5 shows the results. Threshold and slope efficiency are defined with respect to the absorbed pump power. All crystals yielded the highest output power with an output coupler of 1% transmission at 1550 nm. Laser oscillation was also achieved with mirrors of 0.4% and 1.7% transmission at 1550 nm although with less efficiency.

Even at high pump power (2 W) only a very slightly lower efficiency of the cw laser in respect to the quasi cw regime (1:2 duty cycle) had been observed.

The losses due to crystal defects and depolarization were estimated to be approximately 2% for a cavity round trip. Due to a weak green fluorescence in the pumping channel some additional losses must be attributed to upconversion processes into the Er <sup>4</sup>F<sub>7/2</sub> manifold.

The wavelength of the laser emission of Er( $3.0 \times 10^{19} \text{ cm}^{-3}$ ), Yb( $7.7 \times 10^{20} \text{ cm}^{-3}$ ):Sc<sub>2</sub>SiO<sub>5</sub> could be tuned continuously with a birefringent filter between 1524–1534 nm and 1545–1560 nm in X-polarization.

In the free running regime stimulated emission was obtained in Z-polarization although this might be affected by the individual quality of the sample.

## 7.2. Excitation by diodes

The experimental setup for diode pumping was based on two laser diodes (IBM-SU3128C-6) with 2 W maximum power at 968 nm. Their emission spectra had a width of 6 nm and could be temperature tuned by 2 nm. The two emitted beams were combined with a polarizing beam splitter and focused by a lens ( $f = 25 \text{ mm}$ ) to a crosslike spot

combining the elliptical modes of  $120 \mu\text{m} \times 20 \mu\text{m}$  size of each diode. The uncoated crystals were mounted on a water cooled copper block within a hemispherical resonator. The curvature of the output mirror was  $r = 50 \text{ mm}$ .

Laser oscillation in this setup was achieved only with Er( $3.0 \times 10^{19} \text{ cm}^{-3}$ ), Yb( $7.7 \times 10^{20} \text{ cm}^{-3}$ ):Sc<sub>2</sub>SiO<sub>5</sub> in Z-polarization at 1551 nm. The input–output characteristics are shown in Fig. 5. The maximum output power was  $P_{\text{max}} = 24 \text{ mW}$  using again a 1% output coupler. The slope efficiency was  $\eta_{\text{diff}} = 2.4\%$  and the threshold pump power was  $P_{\text{thr}} = 255 \text{ mW}$  while 85% of the total pump power was absorbed. However, the laser efficiency of this sample was higher under diode pumping than under pumping with an Ti:Al<sub>2</sub>O<sub>3</sub> laser ( $\eta_{\text{diff}} = 1.8\%$ ,  $P_{\text{thr}} = 805 \text{ mW}$ ).

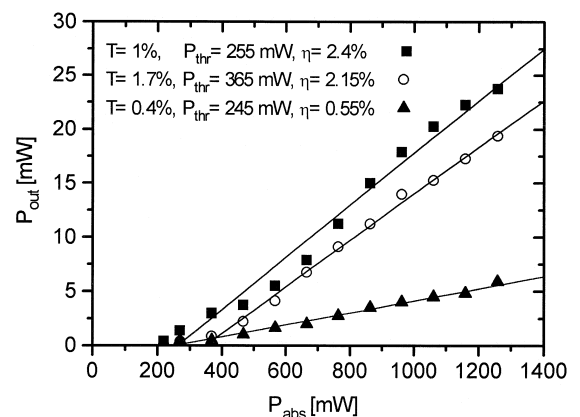


Fig. 5. Output of diode pumped Er( $3.0 \cdot 10^{19} \text{ cm}^{-3}$ ), Yb( $7.7 \times 10^{20} \text{ cm}^{-3}$ ):Sc<sub>2</sub>SiO<sub>5</sub> with 0.4%, 1%, and 1.7% outcoupling at 1.55  $\mu\text{m}$ .

Er,Yb:Sc<sub>2</sub>Si<sub>2</sub>O<sub>7</sub> did not perform lasing in this setup what was probably due to the bad overlapping of the diode emission spectrum and the Yb absorption spectrum. Laser action in this host should be possible with pumping by diodes emitting in the Yb absorption peak at 978 nm.

## 8. Conclusion

Erbium doped Sc<sub>2</sub>SiO<sub>5</sub> and Sc<sub>2</sub>Si<sub>2</sub>O<sub>7</sub> crystals are suitable materials for laser oscillation around 1.55 μm. The peak emission cross sections of Er<sup>3+</sup> on the <sup>4</sup>I<sub>13/2</sub> → <sup>4</sup>I<sub>15/2</sub>-transition are 1.5 × 10<sup>-20</sup> cm<sup>2</sup> in Sc<sub>2</sub>SiO<sub>5</sub> and 4.0 × 10<sup>-20</sup> cm<sup>2</sup> in Sc<sub>2</sub>Si<sub>2</sub>O<sub>7</sub>. The possibility of diode pumping was demonstrated for Sc<sub>2</sub>SiO<sub>5</sub> using Yb<sup>3+</sup> codoping. An output power of 24 mW with a slope efficiency of η<sub>diff</sub> = 2.4% was achieved.

The laser efficiency is comparable to that of other Yb,Er doped silicates. However, the performance is still worse than that of Yb,Er:phosphate glass microchip lasers.

To achieve better results on the Er <sup>4</sup>I<sub>13/2</sub> → <sup>4</sup>I<sub>15/2</sub> transition in crystal hosts a material with high Yb–Er energy transfer rates, low upconversion losses and a large Stark splitting of the ground state is still necessary.

## References

- [1] P. Thony, E. Molva, OSA TOPS on Advanced Solid-State Lasers 1 (1996) 296–300.
- [2] P. Laporta, S. De Silvestri, V. Magni, O. Svelto, Opt. Lett. 16 (24) (1991) 1952–1954.
- [3] P. Laporta, S. Longhi, S. Taccheo, O. Svelto, Opt. Lett. 18 (1) (1993) 31–33.
- [4] W.L. Barnes, P.R. Moekel, L. Reekie, D.N. Payne, Opt. Lett. 14 (18) (1989) 1002–1004.
- [5] P. Laporta, S. Taccheo, S. Longhi, O. Svelto, G. Sacchi, Opt. Lett. 18 (15) (1993) 1232–1234.
- [6] S. Taccheo, P. Laporta, S. Longhi, O. Svelto, C. Svelto, Appl. Phys. B 63 (1996) 425–436.
- [7] K. Spariosu, M. Birnbaum, OSA Proc. Advanced Solid-State Lasers 13 (1992) 127–130.
- [8] T. Schweizer, T. Jensen, E. Heumann, G. Huber, Opt. Comm. 118 (1995) 557–561.
- [9] K. Spariosu, R.D. Stulz, M.B. Camargo, S. Montgomery, M. Birnbaum, B.H.T. Chai, OSA Proc. Advanced Solid-State Lasers 24 (1995) 379–383.
- [10] C. Li, C. Wyong, R. Moncorgé, IEEE J. Quantum Electron. 28 (4) (1992) 1209–1221.
- [11] B. Simondi-Teisseire, B. Viana, A.-M. Lejus, A.-M. Benitez, D. Vivien, C. Borel, R. Templier, C. Wyon, IEEE J. Quantum Electron. 32 (1996) 2004–2009.
- [12] B. Simondi-Teisseire, B. Viana, A.M. Lejus, D. Vivien, C. Borel, R. Templier, C. Wyon, OSA TOPS on Advanced Solid-State Lasers 1 (1996) 301–305.
- [13] J.C. Souriau, R. Romero, C. Borel, Ch. Wyon, C. Li, R. Moncorgé, Opt. Mater. 4 (1994) 133–137.
- [14] A.M. Tkachuk, A.K. Przhhevusskii, L.G. Morozova, A.V. Poletimova, M.V. Petrov, A.M. Korovkin, Opt. Spectrosc. (USSR) 60 (2) (1986) 176–181.
- [15] Strukturbericht, Bd. II, Akad.-Verl. Leipzig, 1937, pp. 124–125.
- [16] H. Klaska, to be published.
- [17] L.D. DeLoach, S.A. Payne, L.L. Chase, L.K. Smith, W.L. Kway, W.F. Krupke, IEEE J. Quantum Electron. 29 (1993) 1179–1190.
- [18] S.A. Payne, L.L. Chase, L.K. Smith, W.L. Kway, W.F. Krupke, IEEE J. Quantum Electron. 28 (11) (1992) 2619–2630.
- [19] J. Rubin, A. Brenier, R. Moncorgé, C. Pedrini, J. Lumin. 36 (1986) 39–47.
- [20] T. Wegner, K. Petermann, Appl. Phys. B 49 (1989) 275.
- [21] S. Zemon, G. Lambert, W.J. Miniscalco, R.W. Davies, B.T. Hall, R.C. Folweiler, T. Wei, L.J. Andrews, M.P. Singh, SPIE 1373, Fiber Laser Sources and Amplifiers, vol. 2, 1990, p. 21.
- [22] J. Koetke, G. Huber, Appl. Phys. B 61 (1995) 151–158.
- [23] E. Heumann, P. Möbert, G. Huber, Exp. Techn. Phys. 42 (1) (1996) 33–38.
- [24] T. Danger, J. Koetke, R. Brede, E. Heumann, G. Huber, B.H.T. Chai, J. Appl. Phys. 76 (3) (1994) 1413–1422.
- [25] D.S. Knowles, H.P. Jenssen, IEEE J. Quantum Electron. 28 (4) (1992) 1197–1208.
- [26] T. Jensen, K. Ostroumov, G. Huber, OSA Proc. Advanced Solid-State Lasers 24 (1995) 366–370.